Binding Energies of Proton-Bound Ether/Alcohol Mixed Dimers Determined by FTICR Radiative Association Kinetics Measurements

Travis D. Fridgen† and Terry B. McMahon*

Department of Chemistry, University of Waterloo, Waterloo, Ontario, Canada, N2L 3G1

Received: October 10, 2001; In Final Form: December 16, 2001

The reactions of protonated diethyl ether with ethanol and protonated di-*n*-propyl ether with *n*-propanol, producing the mixed proton-bound dimers, were studied at low pressures in a FTICR cell. The pressure dependence of the apparent rate constant for proton-bound dimer formation was investigated and yielded unimolecular dissociation rate constants, k_b, and photon emission rate constants, k_{ra}, for the nascent proton-bound dimers at internal energies equal to the dissociation energies of the dimers. The experimental k_{ra} values were found to be 17 ± 3 and 6.3 ± 0.6 s^{-1}, respectively, for the ethanol/diethyl ether and *n*-propanol/di-*n*-propyl ether proton-bound dimers. RRKM modeling of the unimolecular dissociation rate constants as a function of the binding energies yielded the 0 K dissociation energies of the proton-bound dimers as 109 ± 1 and 105.1 ± 0.6 kJ mol^{-1} for the ethanol/diethyl ether and *n*-propanol/di-*n*-propyl ether proton-bound dimers, respectively. Using B3LYP/6-311G** thermal energies, the corresponding 298 K bond strengths were determined to be 103 ± 1 and 99.5 ± 0.6 kJ mol^{-1}. These agree quite well with those predicted by a simple relationship based upon the differences in proton affinities of the neutral monomers. In addition, the association reaction of *n*-propanol with protonated di-*n*-propyl ether reaches what appears to be equilibrium at long reaction times. The relative intensities of the product and reactant ions as well as the pressure of neutral *n*-propanol were used to obtain an equilibrium constant for the reaction of $9.8(\pm 0.9) \times 10^{10}$ at 294 K. From this equilibrium constant and a calculated entropy of reaction of 128 J K^{-1} mol^{-1}, the 294 K bond strength was determined to be 100.3 ± 6.0 kJ mol^{-1}, in excellent agreement with the values determined from the radiative association kinetics and B3LYP/6-311G** calculations.

1. Introduction

Thermochemical data for numerous symmetrical proton-bound cluster ions have been determined by high-pressure mass spectrometry. Temperature dependencies of the equilibrium constants have been shown to give accurate enthalpies and entropies for the clustering reactions

$$A_nH^+ \rightarrow A_{n-1}H^+ + A \quad n = 2,3... \qquad (1)$$

The monomer/dimer equilibria ($n = 2$ in eq 1) of numerous species have been extensively studied, and it has been shown that the symmetric dimers have binding energies that depend, for the most part, only on the heteroatom. For example, symmetrical proton-bound dimers of oxygen *n*-donor bases all have bond strengths of around 129−134 kJ mol^{-1}, whether the monomers be acids, alcohols, aldehydes, esters, ethers, ketones, or water. Similarly, proton-bound dimers of nitrogen *n*-donor bases typically all have bond strengths of around 101−105 kJ mol^{-1}.

While symmetrical proton-bound dimer thermochemistry has been extensively studied, that of unsymmetrical proton-bound dimers has received less attention. This is due to the fact that the bond energies of unsymmetrical proton-bound dimers are typically less than those of symmetrical proton-bound dimers since the proton affinity (PA) of one monomer is greater than the other. This means that if one were to try to study mixed proton-bound dimers, AHB^+, in a high-pressure source by the clustering of two neutral bases, A and B where PA(A) is greater than PA(B), the symmetrical proton-bound dimer AHA^+ would dominate and little if any of AHB^+ might be present unless the partial pressure of species B is much greater than that of A. Despite the experimental difficulties, Hiraoka et al.[1] obtained thermochemical data from temperature-dependent equilibrium studies using high-pressure mass spectrometry for numerous water/dimethyl ether and methanol/dimethyl ether proton-bound clusters by ensuring a large excess of water or methanol, respectively, for the two mixed systems studied.

Larson and McMahon[2] used an ion cyclotron resonance (ICR) mass spectrometer to study 28 mixed proton-bound dimers of oxygen *n*-donor bases. Under the typical low-pressure conditions within the ICR cell, stabilizing collisions are not frequent enough to observe stabilization of the nascent proton-bound dimer. However, using a ternary mixture of the two bases of interest as well as $(CHF_2)_2O$, it was found that equilibrium could be established even at low pressures (10^{-6} Torr). The role of $(CHF_2)_2O$ in the mixture[3] is integral since bimolecular reactions leading to proton-bound dimers are involved. From the measured equilibrium constants and estimated ΔS values, bond energies for the mixed proton-bound dimers were obtained. Their studies showed that the bond energy between a protonated base, AH^+, and a base of lower proton affinity, B, was related to the difference in proton affinities of the bases. This empirical relationship for oxygen *n*-donor bases can be summarized by eq 2:

$$\Delta H^\circ_D = 131(\pm 1) \text{ kJmol}^{-1} - 0.5(\pm 0.1) \times \Delta PA \qquad (2)$$

* To whom correspondence should be addressed. E-mail: mcmahon@uwaterloo.ca.
† E-mail: tdfridge@sciborg.uwaterloo.ca.

10.1021/jp0137569 CCC: $22.00
Published on Web 02/05/2002

SCHEME 1

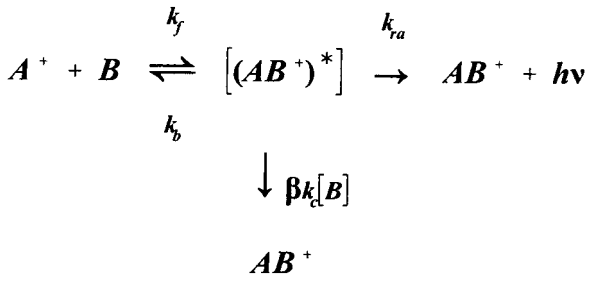

The value 131 kJ mol^{-1} in eq 2 represents the typical bond strength of symmetrical proton-bound dimers of oxygen *n*-donor bases.

Using pulsed high-pressure mass spectrometry, Meot-Ner[4] obtained thermochemical information for 48 mixed proton-bound dimers with $-NH^+\cdots O-$ linkages. A convincing correlation between the difference in proton affinities (ΔPA) of the two bases and the bond dissociation energy ($\Delta H°_D$) between the weaker base and the protonated monomer was also determined (eq 3),

$$\Delta H°_D = 125.5 \pm 6.3 \text{ kJmol}^{-1} - 0.26 \pm 0.03|\Delta PA| \quad (3)$$

Similar correlations were observed for $-NH^+\cdots N-$ bonds in ammonium ion dimers and $-OH^+\cdots O-$ bonds in oxonium ion hydrates and many other types of ionic hydrogen bonds.[2,5]

The observation of ambient temperature blackbody infrared radiation induced dissociation within the low-pressure confines of a Fourier transform ion cyclotron resonance (FTICR) cell revealed a new method for determining bond energies of weakly bound clusters.[6] Master equation modeling is done to simulate the temperature-dependent blackbody infrared radiation induced dissociation kinetics from which activation energies and Arrhenius parameters are determined. The modeled Arrhenius parameters are compared with the experimental values using the threshold dissociation energy, E_o, as a variable. The value of E_o required to successfully reproduce the experimental Arrhenius parameter is then taken as the dissociation energy. Williams and co-workers have exploited this method to determine bond energies of symmetrical and unsymmetrical proton-bound[7,8] and alkali metal-bound dimers[9] of biological importance as well as dimers of deoxyribose nucleotides.[10]

Radiative association kinetics measurements have also been used to determine binding energies for ion/molecule complexes. At very low pressures, the collision between an ion and a molecule results in a nascent complex which is stabilized by emission of an infrared photon or, more rarely at very low pressures, by collision with a third body (Scheme 1).[11]

By applying the steady-state assumption to the concentration of $(AB^+)^*$, an apparent bimolecular rate constant for loss of reactants is given by eq 4.

$$k_{app} = \frac{k_f(k_{ra} + \beta k_c[B])}{k_b + k_{ra} + \beta k_c[B]} \quad (4)$$

By performing a Taylor series expansion about [B] = 0 to first order in [B], it is readily shown that the apparent rate constant for formation of AB^+ is given by eq 5.[11]

$$k_{app} = \frac{k_f k_{ra}}{k_b + k_{ra}} \frac{\beta k_b k_f k_c[B]}{(k_b + k_{ra})^2} \quad (5)$$

If it is assumed that k_{ra} is much smaller than k_b and the strong collision assumption is used ($b = 1$), which are typically good assumptions, eq 5 reduces to eq 6.

$$k_{app} = \frac{k_f k_{ra}}{k_b} + \frac{k_f k_c[B]}{k_b} \quad (6)$$

If it is assumed further that every collision between A^+ and B results in formation of the nascent $(AB^+)^*$ and that every collision between $(AB^+)^*$ and B results in sufficient stabilization of the complex (i.e., $\beta = 1$, the strong collision assumption) to dramatically slow the rate of unimolecular dissociation, then k_f and k_c can be estimated from the calculated collision rate constants. Therefore, by monitoring the depletion of A^+ at various pressures of neutral reactant and plotting the apparent rate constant against pressure of neutral reactant, the rate constants for unimolecular dissociation, k_b, and radiative stabilization, k_{ra}, of the activated complex can be obtained directly from the slope and intercept, respectively. Master equation modeling[12] is performed to simulate k_b with the binding energy of the ion/molecule complex as the only variable. The binding energy is, then, that required to reproduce the experimental k_b from the master equation modeling.

This method has been used by Dunbar's group to obtain binding energies of metal cations to unsaturated hydrocarbons and other organic compounds as well metal cation-bound dimers.[13] Binding energies of symmetrical proton-bound dimers[14] as well as NO^+/3-pentanone[15] and NO^+/iron(II) porphyrin[16] ion/molecule have also been determined by this method.

In the present work we report the radiative association kinetics of the unsymmetrical diethyl ether/ethanol and di-*n*-propyl ether/*n*-propanol proton-bound dimers. Radiative association and unimolecular lifetimes are determined and compared with those calculated by standard methods. Also, Dunbar's method has been used to obtain "experimentally" the binding energies of the two proton-bound dimers.

2. Methods

2.1. Experimental. All experiments were carried out with a Bruker CMS 47 FT-ICR mass spectrometer equipped with a 4.7 T magnet. Vapor from samples of ethanol (100%, Consolidated Alcohols), and *n*-propanol (99.7%, Aldrich) were degassed using a minimum of three freeze−pump−thaw cycles and were introduced into the ICR cell via heated precision leak valves. The pressure inside the vacuum chamber was measured via a calibrated ionization gauge. The calibration factors for pressures of ethanol and propanol were 1.5 and 1.25, respectively, and were determined as described previously.[17]

The pulse sequence used for these experiments is shown in Figure 1. Ionization was done directly inside the ICR cell using ~100 ms pulses of 70 eV electrons. The first delay was incorporated to produce protonated diethyl ether or protonated di-*n*-propyl ether (eqs 7 and 8, respectively) by ethyl cation and *n*-propyl cation exchange, respectively.

$$CH_3CH_2OH_2^+ + CH_3CH_2OH \rightarrow (CH_3CH_2)_2OH^+ + H_2O \quad (7)$$

$$CH_3CH_2CH_2OH_2^+ + CH_3CH_2CH_2OH \rightarrow (CH_3CH_2CH_2)OH^+ + H_2O \quad (8)$$

The kinetics as well as experimental transition-state thermo-

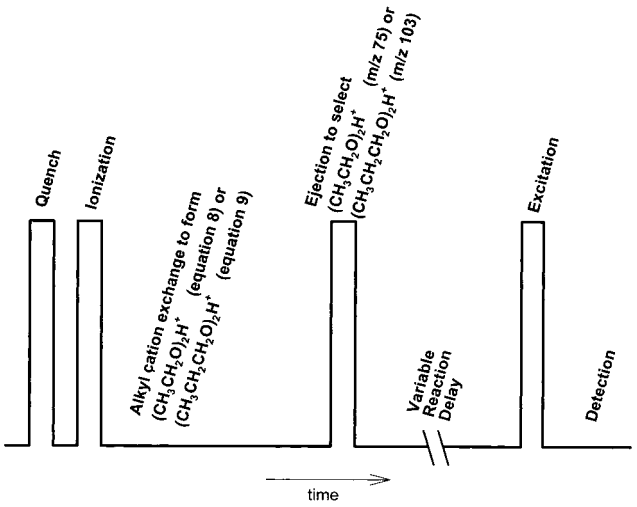

Figure 1. Scan function for the FT-ICR experiments reported in this work.

dynamic parameters for these two processes are reported elsewhere.[17]

After an appropriate period of time for alkyl cation transfer, the ICR cell was quenched of all ions except the desired protonated diethyl ether (*m*/*z* 75) or di-*n*-propyl ether (*m*/*z* 103) by standard rf ejection techniques. The isolated ion was then allowed to react for various periods of time with the neutral background gas, which was either ethanol or *n*-propanol. The rate constants for the association reactions in eqs 9 and 10 were obtained from a least-squares fitting of a semilogarithmic plot of normalized precursor ion intensity vs time.

$$(CH_3CH_2)_2OH^+ + CH_3CH_2OH \rightarrow [(CH_3CH_2)_2O][CH_3CH_2OH]H^+ \quad (9)$$

$$(CH_3CH_2CH_2)_2OH^+ + CH_3CH_2CH_2OH \rightarrow [(CH_3CH_2CH_2)_2O][CH_3CH_2CH_2OH]H^+ \quad (10)$$

Typical mass spectra for reaction 9 are shown in Figure 2 for various reaction times. The corresponding semilogarithmic plot is shown in Figure 3. The reactions were all performed at ambient temperature (294 K).

2.2. Computational. Structures were optimized and vibrational frequencies were calculated at the B3LYP/6-311G** level of theory using the Gaussian 98 suite of programs.[18] The vibrational frequencies were scaled by a factor of 0.95 (ref 19) for use in the RRKM modeling described below.

The dipole-corrected ion/polar molecule rate constants, k_f and k_c (see Scheme 1), were calculated using the trajectory algorithm of Su and Chesnavich.[20] The rate constant for radiative stabilization, k_{ra}, was modeled by standard methods[21] using eq 11[22]

$$k_{ra} = \sum_{i=1}^{N_m}\sum_{n=0}^{\infty} 1.25 \times 10^{-7} n P_i(n) I_i \nu_i^2 \quad (11)$$

Here, the first summation is over the number of normal modes N_m and the second summation is over the number of levels included. The ab initio calculated vibrational wavenumbers υ (in cm^{-1}) and intensities I (in km mol^{-1}) were used since, to date, experimental vibrational wavenumbers and intensities for complex polyatomic ions are virtually nonexistent. The canonical distribution of states, $P_i(n)$, was calculated according to eq 12

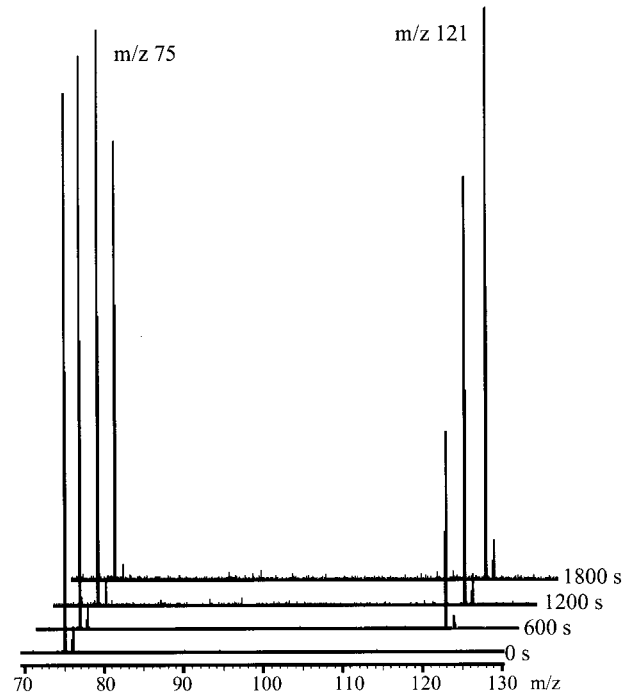

Figure 2. Mass spectra taken after delays of 0, 600, 1200, and 1800 s of reaction between protonated diethyl ehter (*m*/*z* 75) and neutral ethanol conducted at 294 K and an ethanol pressure of 1.3×10^{-8} mbar. Note that the spectra shown at longer delays are offset slightly to higher mass for clarity.

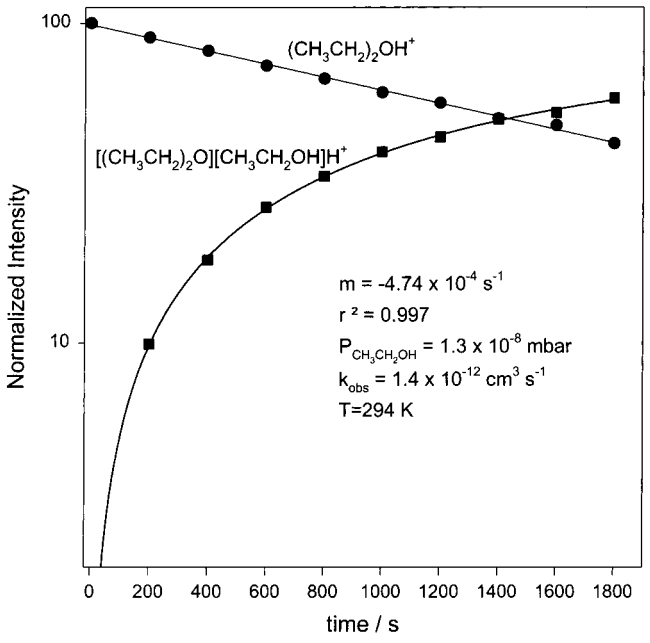

Figure 3. Semilogarithmic plot of intensity vs time for the reaction of protonated diethyl ether with neutral ethanol. The temperature and pressure conditions are the same as those in Figure 2.

$$P_i(n,T)\exp\left(-\frac{h\nu_i n}{k_B T}\right)\left[1-\exp\left(-\frac{h\nu_i}{k_B T}\right)\right] \quad (12)$$

where h and k_B are the Planck and Boltzmann constants, respectively, ν_i are the vibrational frequencies in s^{-1}, and T is the internal temperature of the newly formed dimer calculated

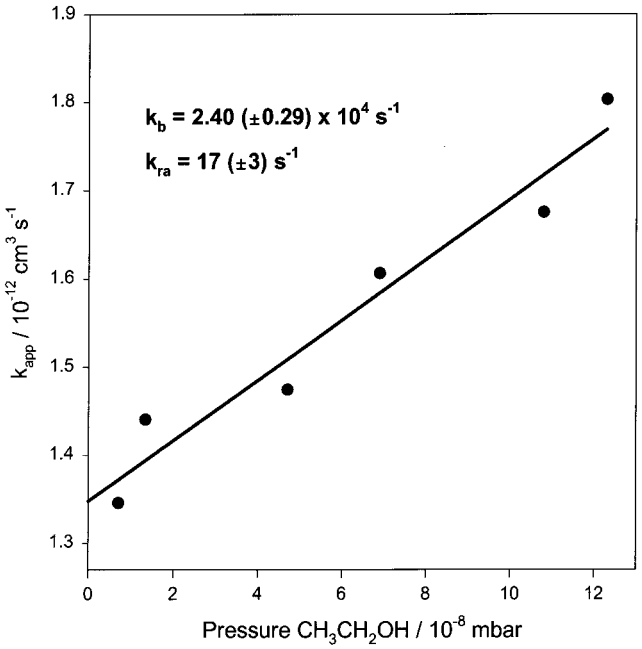

Figure 4. Plot of the apparent rate constant for the formation of the proton-bound dimer of diethyl ether and ethanol vs pressure of neutral ethanol.

by solving the following equation numerically for T

$$E_t = \sum_i \left[\frac{h\nu_i N_A}{e^{h\nu_i/k_B T} - 1} \right] \quad (13)$$

where E_t is the threshold dissociation energy.

Theoretical unimolecular dissociation rate constants were obtained from master equation modeling using the VARIFLEX[23] program, which uses variational transition state theory (VTST) in order to minimize the RRKM unimolecular dissociation rate constant due to the absence of a well-defined transition state structure for dissociation. The B3LYP/6-311G** calculated geometries, vibrational wavenumbers, and intensities were employed for these calculations.

3. Results and Discussion

3.1. Protonated Diethyl Ether/Ethanol. The reaction of protonated diethyl ether with ethanol produced only the mixed proton-bound dimer. The observed rate constant for formation of the proton-bound dimer versus pressure of neutral ethanol is shown in Figure 4. As expected, the observed rate constant for formation of the proton-bound dimer increases with increasing pressure due to an increase in the third-body stabilization rate. However, at zero pressure the rate constant is nonzero due to stabilization of the nascent ion/molecule complex by the process of emission of an infrared photon, or radiative association. The slope and intercept of the plot in Figure 4 are given in Table 1. Using the calculated ion/polar molecule collision rate constants (Table 1) and using eq 6, the unimolecular rate constants for dissociation of the nascent ion/molecule complex, k_b, and for radiative association, k_{ra}, are determined. These are also given in Table 1.

The rate constant for radiative association was found to be 17 ± 3 s^{-1}. The calculated rate constant, calculated using eqs 11−13, is 24 s^{-1}, which is only slightly higher than the experimental value. We[24] have attributed the disagreement between experimental and calculated values of k_{ra} as being due to the fact that, to calculate k_{ra}, ab initio estimates of the vibrational frequencies and intensities are required. Since these calculated frequencies and intensities are those characteristic of the $0 \leftarrow 1$ transition for an internally cool dimer, they cannot be expected to be the same as the frequencies and intensities for the nascent dimer, which is energetically at the dissociation threshold with ~100 kJ mol^{-1} of internal energy.

TABLE 1: Summary of Rate Constants for the Protonated Ether/Alcohol Association Reactions

	Et_2OH^+/EtOH	Pr_2OH^+/PrOH
slope/10^{-22} cm^6 s^{-1}	1.39 ± 0.16	7.99 ± 0.69
intercept/10^{-12} cm^3 s^{-1}	1.35 ± 0.10	3.21 ± 0.11
k_f/10^{-9} cm^3 s^{-1} (calc)[a]	1.90	1.68
k_c/10^{-9} cm^3 s^{-1} (calc)[a]	1.75	1.56
k_b/10^3 s^{-1}	24.0 ± 2.9	3.28 ± 0.28
k_{ra}/s^{-1}	17 ± 3	6.3 ± 0.6
k_{ra} (calc)/s^{-1}	24	11
τ_b/μs	42 ± 5	305 ± 26
τ_{ra}/ms	59 ± 10	159 ± 15
correlation (r)[b]	0.973	0.982

[a] Dipole-corrected ion−neutral collision rate constants. [b] Least-squares fit of slope and intercept.

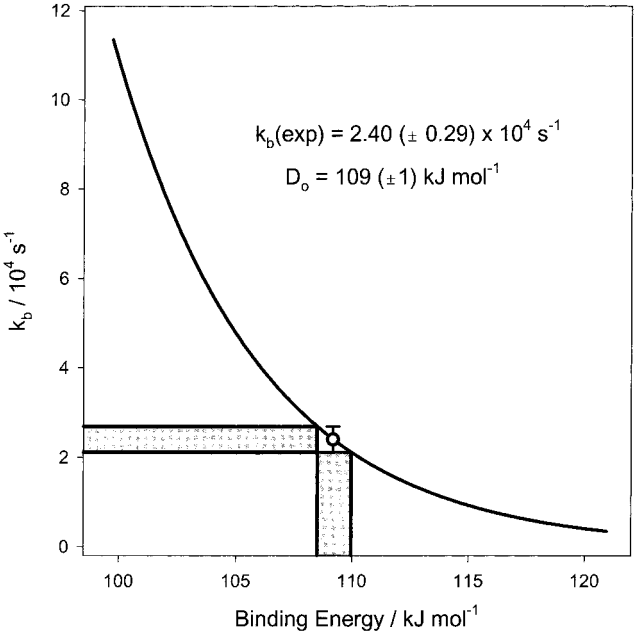

Figure 5. Plot of the RRKM-calculated unimolecular dissociation rate constant of the nascent proton-bound dimer of diethyl and ethanol at various internal energies.

The unimolecular dissociation rate constant for the nascent diethyl ether/ethanol proton-bound dimer was determined to be 2.40 (±0.29) × 10^4 s^{-1}. Unimolecular dissociation rate constants were calculated as a function of binding energy E_o and the plot of the calculated k_b vs E_o is shown in Figure 5. As outlined by Dunbar,[13−15] the binding energy required to reproduce the experimental unimolecular rate constants was taken as the binding energy of the proton-bound dimer. The 0 K binding energy was determined to be 109 ± 1 kJ mol^{-1}. The calculations performed at the B3LYP/6-311G** level of theory result in a 0 K binding energy of 114.6 kJ mol^{-1}, in very good agreement with our experimental value.

3.2. Protonated Di-*n*-Propyl Ether/*n*-Propanol. The reaction between protonated di-*n*-propyl ether and *n*-propanol was slightly more complicated than that of the ethyl analogue described above. It was not possible to isolate protonated di-*n*-propyl ether at *m*/*z* 103 exclusively, due to the presence of a species at *m*/*z* 101 which could be due to a loss of H_2 from *m*/*z*

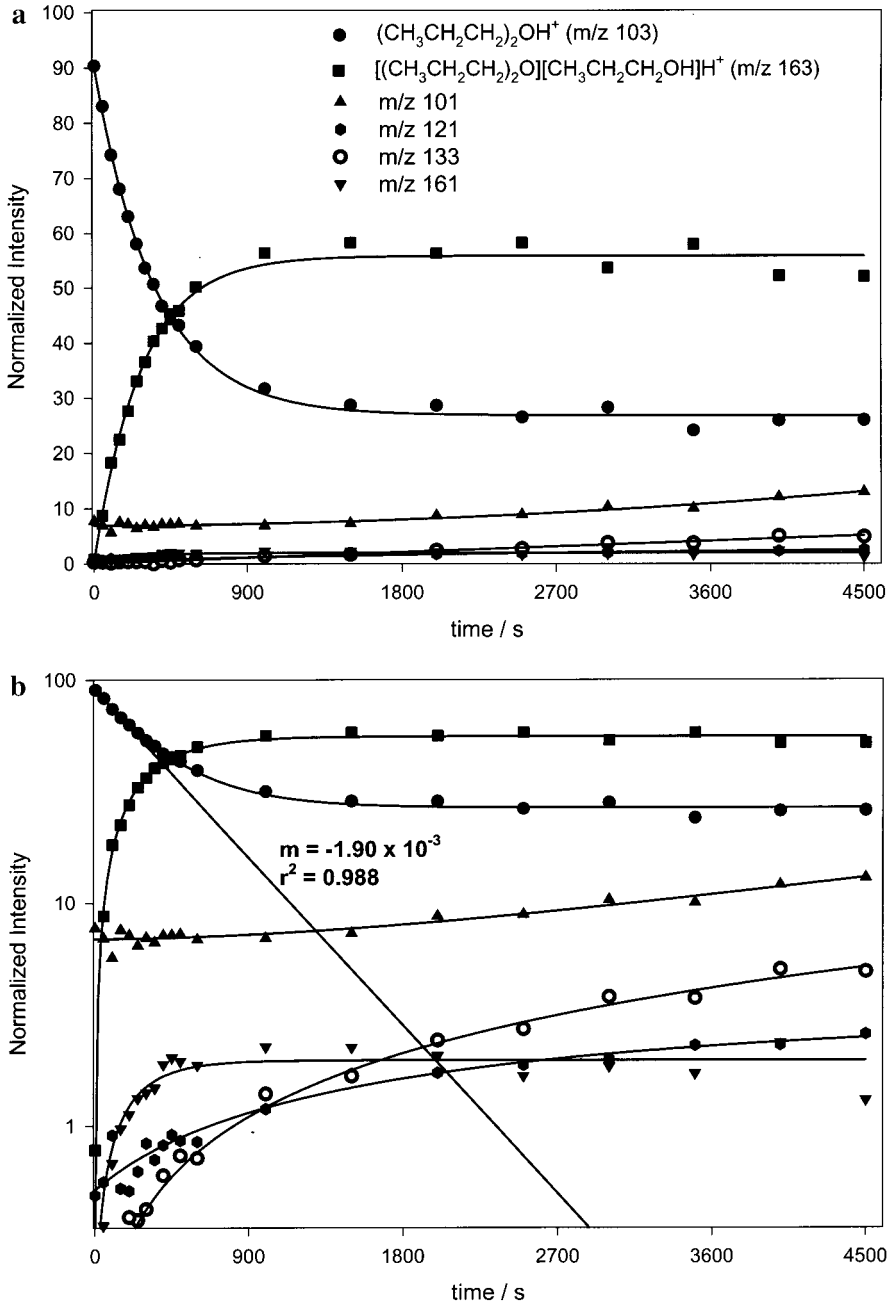

Figure 6. (a) Plot of intensities of ions vs time for the reaction of protonated di-*n*-propyl ether with *n*-propanol conducted at 298 K and a 2.2×10^{-8} mbar of neutral *n*-propanol. (b) Semilogarithmic plot of intensity vs time for the reaction of protonated diethyl ether with neutral ethanol showing the slope of the line used to determine the apparent rate constant for proton-bound dimer formation.

103 following the *n*-propyl cation exchange reaction. This reaction is roughly 30 kJ mol^{-1} exothermic beginning with *n*-propanol and protonated *n*-propanol according to B3LYP/6-31+G* calculations. Therefore, both *m*/*z* 101 and 103 were present prior to the start of the kinetics experiment as is evident from Figure 6. As well, very minor products at *m*/*z* 121, *m*/*z* 133, and *m*/*z* 161 grow in at longer times. The product at *m*/*z* 161 is presumably due to clustering of *n*-propanol onto *m*/*z* 101. The peak at *m*/*z* 121 cannot be due to the proton-bound dimer of *n*-propanol formed by exchange of di-*n*-propyl ether for *n*-propanol. The proton-bound dimer of *n*-propanol is expected to be more strongly bound than the mixed proton-bound dimer (see below); however, the proton affinity of di-*n*-propyl ether is much greater than that of *n*-propanol (837.9 versus 786.5 kJ mol^{-1}), such that the exchange reaction would be far too endothermic to be plausible. Rather, *m*/*z* 121 is most likely a product of a reaction between protonated di-*n*-propyl ether and *n*-propanol which loses propene (eq 14).

$$(n\text{-}C_3H_7)_2OH^+ + n\text{-}C_3H_7OH \rightarrow (n\text{-}C_3H_7)_2OH{\cdot}H_2O^+ + C_3H_6 \quad (14)$$

The product at *m*/*z* 133 is most likely due to loss of ethane from the nascent proton-bound dimer of *n*-propanol and di-*n*-propyl ether, but this will be discussed further below. These products are present at only about one to two percent of the total ion population and do not affect the kinetics appreciably.

Also apparent from Figure 6a is the observation that the reaction between protonated di-*n*-propyl ether and *n*-propanol does not go to completion over the time observed (4500 s). This is due to equilibrium being established between association of

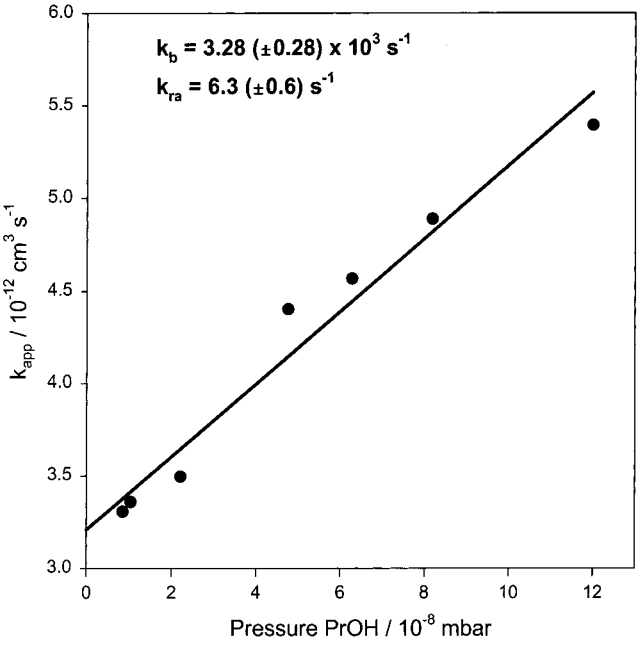

Figure 7. Plot of the apparent rate constant for the formation of the proton-bound dimer of di*n*-propyl ether and *n*-propanol vs pressure of neutral *n*-propanol.

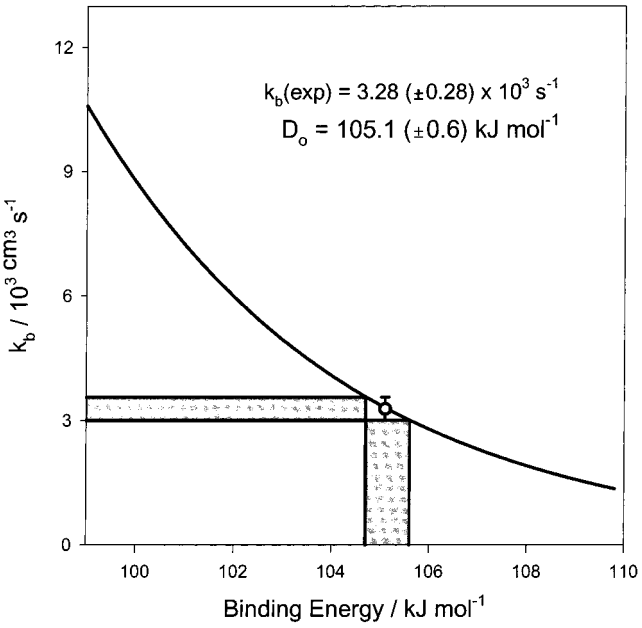

Figure 8. Plot of the RRKM-calculated unimolecular dissociation rate constant of the nascent proton-bound dimer of di-*n*-propyl and *n*-propanol at various internal energies.

protonated di-*n*-propyl ether and *n*-propanol and the reverse dissociation of the proton-bound dimer. The equilibrium will be discussed further below, but it is important to note that the apparent rate constant for proton-bound dimer formation is determined only from the first two hundred to three hundred seconds of reaction (initial rates) due to the complicating equilibrium.

The observed apparent rate constants for proton-bound dimer formation are plotted against the pressure of neutral *n*-propanol in Figure 7. The radiative association rate constant was determined to be 6.3(±0.6) s^{-1} which agrees quite well with the theoretical rate constant, which was calculated to be 11 s^{-1}. The *n*-propanol/di-*n*-propyl ether proton-bound dimer obviously has more degrees of freedom which are able to emit than the ethanol/diethyl ether proton-bound dimer, but both proton-bound dimers have only one very intense infrared mode (> 3000 km mol^{-1}) corresponding to the motion of the proton oscillating between the two monomers. This is the mode that contributes most significantly to the photon-emission rate. The smaller value of k_{ra} for the *n*-propanol/di-*n*-propyl ether proton-bound dimer is expected since it has a significantly lower internal temperature, 520 K vs 640 K for the ethanol/diethyl ether proton-bound dimer (eq 14), due to the 27 additional vibrational modes.

The unimolecular dissociation rate constant was determined to be 3.28 (±0.28) × 10^3 s^{-1}. In the same way as above for the protonated diethyl ether/ethanol system, the binding energy for the proton-bound dimer of di-*n*-propyl ether and *n*-propanol was determined to be 105.1 ± 0.6 kJ mol^{-1} (Figure 8). The B3LYP/6-311G** calculated value for the binding energy was found to be 112.0 kJ mol^{-1}, also in very good agreement with the experimental value.

3.3. Bond Strengths. The binding energies derived from the radiative association experiments are in good agreement with the ab initio values. Nevertheless, it is of obvious interest to compare the experimental values of the binding energies determined here to those determined by other experimental methods. To our knowledge, however, neither the binding energies nor the bond strengths[25] for the proton bound ether/alcohol systems discussed here have been previously reported.

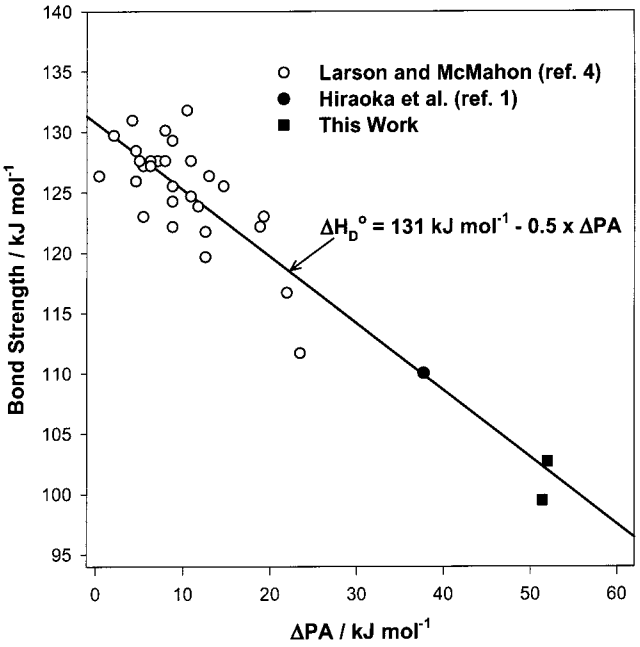

Figure 9. Plot of bond strength of unsymmetrical proton-bound dimers vs the difference in proton affinities of the monomers. The linear relationship shown between the bond strength and difference in proton affinities was determined using only the data from Larson and McMahon[2] (open circles).

As stated above, Larson and McMahon[2] derived an empirical relationship between the mixed proton-bound dimer bond strengths and the difference in proton affinities of the two monomers. This relationship was given above in eq 2. The data from Larson and McMahon[2] has been plotted in Figure 9 along with the linear relationship given by eq 2. To compare the experimental values with the relationship shown in Figure 9, our 0 K binding energies must be converted to 298 K bond strengths. The B3LYP/6-311G** calculated thermochemistry was used for this correction. The difference in total thermal energies for the reactions in eq 10 and 11 were calculated to be 6.3 and 5.6 kJ mol^{-1}, respectively. Using these corrections, the

TABLE 2: Results of Equilibrium Experiments for the Reaction of Protonated Di-*n*-Propyl Ether with *n*-Propanol

pressure *n*-PrOH[a]	I_{163}/I_{103}	$k_{eq}(294)/10^{10}$	$\Delta G_{294}°$/kJ mol^{-1}	$\Delta H°$/kJ mol^{-1} [b]
1.0×10^{-8}	1.06 ± 0.02	10.3 ± 0.2	-62.8 ± 1.2	-100.4 ± 1.2
2.2×10^{-8}	2.02 ± 0.13	9.3 ± 0.6	-62.6 ± 4.0	-100.2 ± 4.0
4.4×10^{-8}	4.65 ± 0.33	9.9 ± 0.7	-62.7 ± 4.5	-100.3 ± 4.5
		9.8 ± 0.9	-62.7 ± 6.0	-100.3 ± 6.0

[a] In mbar. [b] Assuming a $\Delta S°$ for the reaction to be 128 J K^{-1} mol^{-1} (calculated B3LYP/6-311G**).

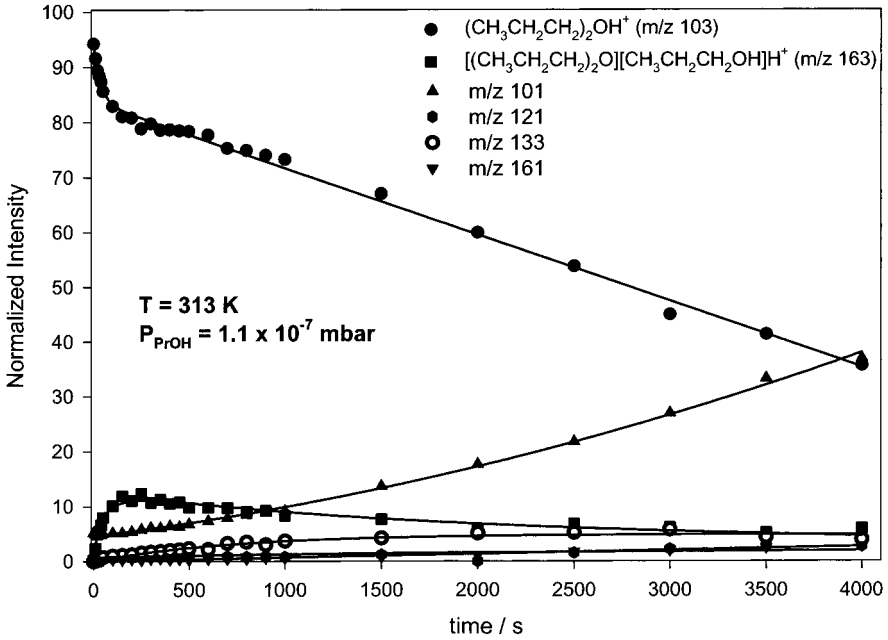

Figure 10. Plot of intensities of ions vs time for the reaction of protonated di-*n*-propyl ether with *n*-propanol conducted at 313 K and a 1.1×10^{-7} mbar of neutral *n*-propanol.

bond strengths are 103 ± 1 and 99.5 ± 0.6 kJ mol^{-1} for the ethanol/diethyl ether and *n*-propanol/di-*n*-propanol proton-bound dimers, respectively, and these values are plotted against the corresponding differences in proton affinities in Figure 9 as well. Also in Figure 9 are the data for the proton-bound dimer of methanol and dimethyl ether.[1] The 298 K bond strengths determined here are, in fact, in excellent agreement with the expected values based on the differences in proton affinities.

3.4. Equilibrium in Protonated Di-*n*-Propyl Ether/*n*-Propanol System. It is evident from Figure 6a,b that a steady state has been established for the reaction of protonated di-*n*-propyl ether with *n*-propanol at long reaction times. Equilibrium in low pressure radiative association studies has been observed previously in the reaction of NO with iron(II) porphyrins[16] and for the hydration reaction of protonated 18-crown-6.[26] The steady-state ratio of *m*/*z* 163 to *m*/*z* 103 (I_{163}/I_{103}) is 2.02×0.13 for the experiment conducted at a neutral *n*-propanol pressure of 2.2×10^{-8} mbar. Experiments were also conducted at neutral pressures of 1.0×10^{-8} and 4.4×10^{-8} mbar with I_{163}/I_{103} values of 1.06 ± 0.02 and 4.65 ± 0.33. These values of I_{163}/I_{103} together with the respective pressures yield equilibrium constant values shown in Table 2. Assuming an entropy change associated with this reaction of 128 J K^{-1} mol^{-1}, which was the value from B3LYP/6-311G** calculations, the equilibrium experiments yield a 294 K bond strength of 100.3 ± 6.0 kJ mol^{-1}, which is in excellent agreement with the value obtained from the radiative association kinetics, 99.5 ± 0.6 kJ mol^{-1} and the B3LYP/6-311G** value of 106.4 kJ mol^{-1}.

It can be seen from Figure 6 that the species at *m*/*z* 133 increases slightly, to roughly 4% of the total ion population over the course of the experiment. Similarly, *m*/*z* 101 increases slightly in intensity over the 4500 s observation time. A number of experiments were conducted at elevated temperatures, and it was found that even after 4500 to 5000 s equilibrium could not be established. In Figure 10 are shown the intensity profiles for all ions observed vs time for the experiment conducted at 313 K. It is evident that protonated di-*n*-propyl ether and the proton-bound dimer of *n*-propanol do not reach equilibrium. Also, *m*/*z* 133 grows in to roughly the same intensity as in the 294 K experiment (Figure 6), but the ion responsible for *m*/*z* 101 grows in much faster than in the 294 K experiment and actually becomes the dominant ion after 4000 s. The ions at *m*/*z* 101 and *m*/*z* 133 are not likely to be products of reaction between *n*-propanol and protonated di-*n*-propyl ether, since their intensities do not begin to increase immediately after zero time. Rather, the ions begin to increase in intensity after the accumulation of some *m*/*z* 163, the proton-bound dimer of *n*-propanol and di-*n*-propyl ether. The production of *m*/*z* 133 and *m*/*z* 101, therefore, is most likely a product of a series of unimolecular decomposition reactions beginning with the thermalized proton-bound dimer. As the temperature increases the rate of formation of *m*/*z* 101 increases, indicating that there is at least a slight barrier along the pathway from *m*/*z* 163 to *m*/*z* 101. Since there is little accumulation of *m*/*z* 133 it is likely that the bottleneck is the decomposition of *m*/*z* 163 to form *m*/*z* 133, which then undergoes a more facile decomposition to form *m*/*z* 101. A possible mechanism for this reaction is shown in Scheme 2.

4. Conclusions

The reactions of protonated diethyl ether with ethanol and protonated di-*n*-propyl ether with *n*-propanol, producing the mixed proton-bound dimers, were studied at low pressures in

SCHEME 2

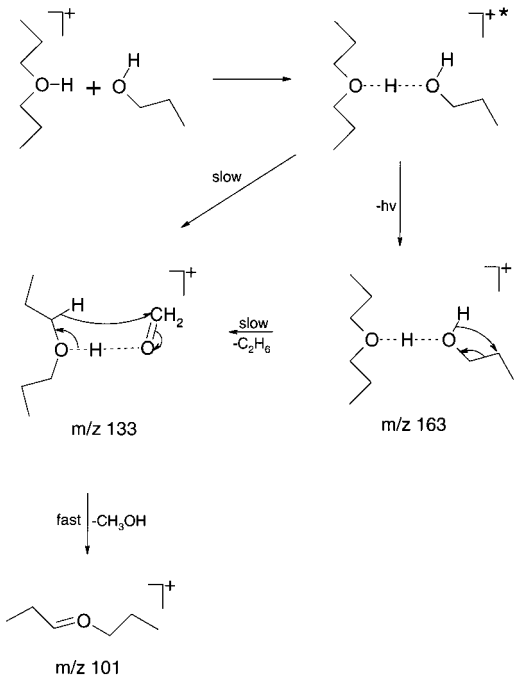

the FTICR cell. The pressure dependence of the apparent rate constants for proton-bound dimer formation yielded unimolecular dissociation rate constants and photon emission rate constants for the proton-bound dimers at internal energies equal to the dissociation energies of the dimers. RRKM modeling of the unimolecular dissociation rate constants as a function of the binding energies yielded the 0 K dissociation energies of the proton-bound dimers, which were found to be 109 ± 1 and 105.1 ± 0.6 kJ mol^{-1} for the ethanol/diethyl ether and *n*-propanol/di-*n*-propyl ether proton-bound dimers, respectively. Using B3LYP/6-311G** thermal energies, the bond strengths were determined to be 103 ± 1 and 99.5 ± 0.6 kJ mol^{-1} for the ethanol/diethyl ether and *n*-propanol/di-*n*-propanol proton-bound dimers, respectively, which agree quite well with those predicted by a simple empirical relationship based upon the differences in proton affinities of the neutral monomers.

The reaction of *n*-propanol with protonated di-*n*-propyl ether reaches equilibrium at longer times than those used for determining association rate constants. The relative intensities of the product and reactant ions as well as the pressure of neutral *n*-propanol were used to obtain an equilibrium constant for the reaction of $9.8 (\pm 0.9) \times 10^{10}$ at 294 K. From the equilibrium constant and a calculated entropy of reaction, the 294 K bond strength was determined to be 100.3 ± 6.0 kJ mol^{-1}, in excellent agreement with the values determined from the radiative association kinetics (99.5 ± 0.6 kJ mol^{-1}) and B3LYP/6-311G** calculations (106.4 kJ mol^{-1}). A temperature dependence on the equilibrium constant was not possible since at all temperatures above ambient (294 K) equilibrium could not be established due to a competing reaction producing *m*/*z* 101, likely formed by the loss of methanol through an intermediate *m*/*z* 133 ion, which likely is a proton-bound dimer of di-*n*-propyl ether and formaldehyde formed by loss of ethane from the proton bound dimer of *n*-propanol and di-*n*-propyl ether.

Acknowledgment. The financial support of the Research Grants Program of the Natural Sciences and Engineering Research Council of Canada (NSERC) is acknowledged. T.D.F. gratefully acknowledges the Posdoctoral Fellowship granted by NSERC.

References and Notes

(1) Hiraoka, K.; Grimsrud, E. P.; Kebarle, P. *J. Am. Chem. Soc.* **1974**, *96*, 3359.

(2) Larson, J. W.; McMahon, T. B. *J. Am. Chem. Soc.* **1982**, *104*, 6255.

(3) Clair, R. L.; McMahon, T. B. *Can. J. Chem.* **1980**, *58*, 863.

(4) Meot-Ner, M. *J. Am. Chem. Soc.* **1984**, *106*, 1257.

(5) Speller, C. V.; Meot-Ner, M. *J. Phys. Chem.* **1985**, *89*, 5217.

(6) Thölmann, D.; Tonner, D. S.; McMahon, T. B. *J. Phys. Chem.* **1994**, *98*, 2002.

(7) Jockusch, R. A.; Williams, E. R. *J. Phys. Chem. A* **1998**, *102*, 4543.

(8) Price, W. D.; Schnier, P. D.; Williams, E. R. *J. Phys. Chem. B* **1997**, *101*, 664.

(9) Schnier, P. D.; Price, W. D.; Strittmatter, E. F.; Williams, E. R. *J. Am. Soc. Mass Spectrom.* **1997**, *8*, 771.

(10) Strittmatter, E. F.; Schnier, P. D.; Klassen, J. S.; Williams, E. R. *J. Am. Soc. Mass Spectrom.* **1999**, *10*, 1095.

(11) Bass, L. M.; Kemper, P. R.; Anicich, V. G.; Bowers, M. T. *J. Am. Chem. Soc.* **1981**, *103*, 5283.

(12) The approach to obtaining binding energies from radiative association kinetics and master equation modeling is best described in Klippenstein, S. J.; Yang, Y.-C.; Rhyzhov, V.; Dunbar, R. C. *J. Chem. Phys.* **1996**, *104*, 4502.

(13) (a) Dunbar, R. C.; Klippenstein, S. J.; Hršák, J.; Stöckigt, D.; Schwarz, H. *J. Am. Chem. Soc.* **1996**, *118*, 5277. (b) Lin, C.-Y.; Dunbar, R. C. *Organometallics* **1997**, *16*, 2691. (c) Ho, Y.-P.; Yang, Y.-C.; Klippenstein, S. J.; Dunbar, R. C. *J. Phys. Chem. A* **1997**, *101*, 3338. (d) Rhyzov, V.; Dunbar, R. C. *J. Am. Chem. Soc.* **1999**, *121*, 2259. (e) Gapeev, A.; Yang, C.-N.; Klippenstein, S. J.; Dunbar, R. C. *J. Phys. Chem. A* **2000**, *104*, 3246. (f) Gapeev, A.; Dunbar, R. C. *J. Phys. Chem. A* **2000**, *104*, 4084.

(14) Rhyzov, V.; Yang, Y.-C.; Klippenstein, S. J.; Dunbar, R. C. *J. Phys. Chem. A* **1998**, *102*, 8865.

(15) Rhyzov, V.; Klippenstein, S. J.; Dunbar, R. C. *J. Am. Chem. Soc.* **1996**, *118*, 5462.

(16) Chen, O.; Groh, S.; Liechty, A.; Ridge, D. P. *J. Am. Chem. Soc.* **1999**, *121*, 11910.

(17) Fridgen, T. D.; McMahon, T. B. *J. Phys. Chem. A*, accepted for publication.

(18) Frisch, M. J.; Trucks, G. W.; Schlegel, H. B.; Scuseria, G. E.; Robb, M. A.; Cheeseman, J. R.; Zakrzewski, V. G.; Montgomery, J. A.. Jr.; Stratmann, R. E.; Burant, J. C.; Dapprich, S.; Millam, J. M.; Daniels, A. D.; Kudin, K. N.; Strain, M. C.; Farkas, O.; Tomasi, J.; Barone, V.; Cossi, M.; Cammi, R.; Mennucci, B.; Pomelli, C.; Adamo, C.; Clifford, S.; Ochterski, J.; Petersson, G. A.; Ayala, P. Y.; Cui, Q.; Morokuma, K.; Malick, D. K.; Rabuck, A. D.; Raghavachari, K.; Foresman, J. B.; Cioslowski, J.; Ortiz, J. V.; Baboul, A. G.; Stefanov, B. B.; Liu, G.; Liashenko, A.; Piskorz, P.; Komaromi, I.; Gomperts, R.; Martin, R. L.; Fox, D. J.; Keith, T.; Al-Laham, M. A.; Peng, C. Y.; Nanayakkara, A.; Gonzalez, C.; Challacombe, M.; Gill, P. M. W.; Johnson, B.; Chen, W.; Wong, M. W.; Andres, J. L.; Gonzalez, C.; Head-Gordon, M.; Replogle, E. S.; Pople, J. A. Gaussian 98, rev A.7; Gaussian, Inc.: Pittsburgh, PA, 1998.

(19) Scott, A. P.; Radom, L. *J. Phys. Chem.* **1996**, *100*, 16502.

(20) Su, T.; Chesnavich, W. J. *J. Chem. Phys.* **1982**, *76*, 5183.

(21) Shi, J.; Bernfeld, D.; Barker, J. R. *J. Chem. Phys.* **1988**, *88*, 6211.

(22) Klippenstein, S. J.; Yang, Y.-C.; Ryzhov, V.; Dunbar, R. C. *J. Chem. Phys.* **1996**, *104*, 4502.

(23) VARIFLEX, version 1.00 Klippenstein, S. J.; Wagner, A. F.; Dunbar, R. C.; Wardlaw, D. M.; Robertson S. H., July 16, 1999.

(24) Fridgen, T. D.; McMahon, T. B. *J. Phys. Chem. A* **2001**, *105*, 1011.

(25) The binding energies derived from the radiative association kinetics are 0 K values while the bond strengths are, as reported here, 298 K values, which are the negative of the enthalpy changes for the reactions in eqs 10 and 11.

(26) Ryzhov, V.; Dunbar, R. C. *J. Am. Soc. Mass Spectrom.* **1999**, *10*, 862.